Laser Bathymetry in the Netherlands

G.J. Kunz, C.W. Lamberts, G.W.M. van Mierlo, F.P.P. de Vries

TNO Physics and Electronics Laboratory
P.O. Box 96864 - 2509 JG The Hague - The Netherlands

H. Visser, C. Smorenburg

TNO Institute of Applied Physics

D. Spitzer, H. Hofstraat

Dutch Ministry of Transport and Public Works, Tidal Waters Division

R.W.J. Dirks

Netherlands Institute for Sea Research (NIOZ, IMOU)

ABSTRACT

Four institutes were involved in a common program to study the potentials of an airborne laser bathymetry system. Apart from the determination of the water depth, a laser bathymetry system can also be applied for measuring the scattering properties of the water and for obtaining information on the water surface. The optical path from the sensor to the bottom was used as a guideline for describing the contributions of the different media and interfaces. The influence of the air-water interface was studied by introducing an ad hoc model for the water surface. This wind driven model includes capillary and gravity waves. To study the system performance, simulations were carried out for different water properties, different sensor altitudes and different system sensitivities. A system consisting of a dual wavelength scanning part (green and infrared) and a fixed infrared part has been proposed to measure the water depth together with the actual water level respectively the average water level. An opto-mechanical scanner design with two rotating wedges promises a flexible scan pattern. Finally the requirements were studied for analog and digital signal processing, data acquisition and in- and after flight data processing.

INTRODUCTION

Laser bathymetry has a large potential for cost-effective depth profiling and water quality monitoring. Therefore, the Dutch Ministry of Transport and Public Works initiated a study on the application of laser bathymetry in the Dutch coastal waters. This study was performed by a consortium of four Dutch institutes (TNO-FEL, TNO-TPD, RWS and NIOZ). The results of the study were reported by Dirks et al (1989) and are summarized in this paper. The optical path from the laser to the bottom and back to the receiver, was the guide for partitioning this project. Furthermore a system design has been suggested based on a three beam configuration and a stabilized opto-mechanical scanner. Signal processing requirements have been studied extensively because the final results depend strongly on in- and after flight processing of the huge amount of data.

1. THE PHYSICS

1.1 The atmosphere

The atmosphere attenuates both the emitted laser beam and the reflected optical signal. The extinction varies from less than 2E-2 km^{-1} for a very clean atmosphere (pure Rayleigh scattering) to about 50 km^{-1} for visibilities as low as 60 m. Although the extinction varies with wavelength and altitude, the extinction profile is not important for bathymetry operation. If the visibility is better than 1 km and the platform altitude is less than 300 m the transmission losses are less than 50 %.

Atmospheric backscatter on the other hand increases as the visibility decreases. Although this backscatter is not of

direct influence on the bathymetry signal, it might reach levels which saturate the receiver temporarily thus masking the signal from the bottom.

Reflections from sunlit aerosols, e.g., from haze and mist layers beneath the sensor, will generate detector background noise. The amount of background radiation can be calculated and depends on the field of view of the receiver, the width of the optical filter and the altitude of the sensor (Appendix).

In addition, the presence of fog layers may reduce the accuracy of the measurements due to pulse broadening caused by muitiple scattering. This effect becomes stronger when the field of view of the receiver becomes larger than the divergence of the laser beam as described by Bucher (1973), Stotts (1978), Matter 1981) and Hughes (1984).

1.2 The water surface

The water surface has been described extensively by a large number of authors, e.g., Cox and Munk (1954), Wu (1971), Schau (1978), Bobb (1979), McClain (1982) and Haimbach and Wu (1986). All authors, however, describe the waves in a statistical way as either slopes or frequency distributions. Descriptions of the actual shape of the surface have not been found, even in one dimension. Therefore the water surface has been simulated by a number of cycloids with a shape factor and an obliqueness factor as suggested e.g. by Groen and Dorrestein (1976) for gravity waves. Additional information for the amplitudes and the shapes of the individual waves has been given by Chang (1978) and Bobb (1979). A combination of four spectral components from the gravity wave spectrum and three components from the capillary wave spectrum, each with different shape factors and phases, has been used to simulate wind driven water surfaces. An example of such a one dimensional water surface, for a wind speed of 5 m/s, is shown in Figure 1 (capillary waves not resolved).
Due to the water waves the optical power distribution over the refracted beam will vary, the illuminated spot over the bottom becomes larger and the uncertainty in the determination of the water depth increases. Simulations show that dispersions as large as 1.5 m are possible. The associated errors in the inverted water depth depend on the algorithm being used to localize the bottom reflection. The effect of the wavy water surface, on both the transmitted and the reflected light, has been studied by means of ray tracing. In Figure 2 the reflected beam, the transmitted beam, the spread of the laser spot over the bottom and the shape of the reflected light pulse from the bottom are shown for a

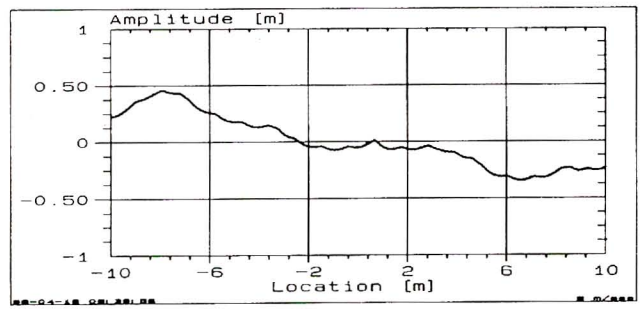

Fig. 1 - A simulated one dimensional water surface for a wind speed of 5 m/s, calculated from four spectral components of the gravity wave spectrum and three spectral components from the capillary wave spectrum with different shape factor and different phases. The capillary waves are not resolved.

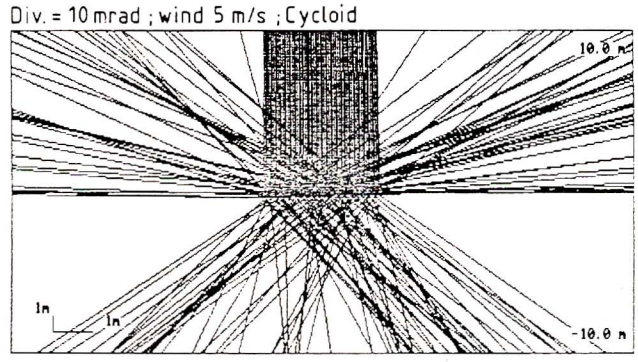

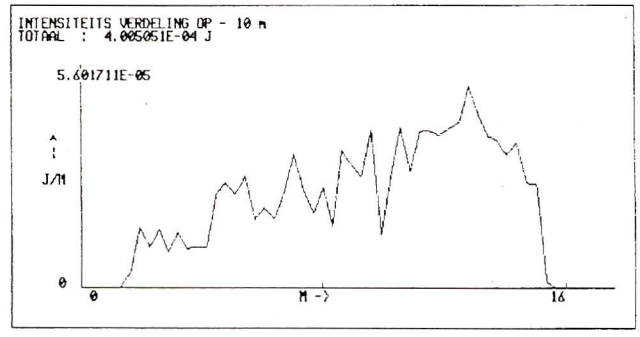

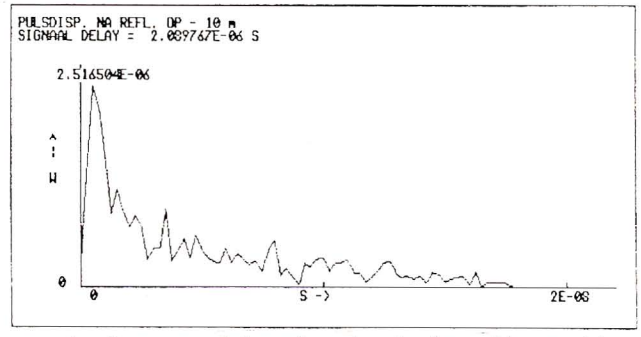

Fig. 2 - Geometry of the reflected and refracted beam with an initial divergence of 10 mrad on a simulated water surface at a wind speed of 5 m/s. The energy distribution over the bottom and the pulse shape of the bottom reflection are presented in the middle and bottom figure.

wind speed of 5 m/s. The calculations indicate that the size of the illuminated spot on the bottom is significantly larger than the original beam and that the pulse reflected from the bottom is spread over at least 10 ns.

Another effect caused by the wavy surface is the strong variation in the reflection of the air-water interface. The equivalent diffuse reflection coefficient of the water surface varies from smaller than 0.02 to larger than 1.5, due to specular reflections. The exact value depends on the sea state and the viewing angle of the system with respect to the vertical. As a result of the time and space varying water level, it is difficult to determine the exact average water level which serves as a reference for the depth. The spread in time of the light pulse reflected off the water surface can be as large as several tens of nanoseconds (equivalent with several meters). On the base of geometrical optics and a maximum slope of the water of 30 degrees, a depth bias of 3.6 % of the actual depth can be expected.

The water surface also reflects the light from natural sources and generates noise in the detector. In overcast situations part of the sky glint enters the receiver via the water surface. The amount of background radiation can be calculated from the sky radiance (Zaha, 1972), the water equivalent diffuse reflection coefficient (Jerlov, 1976, Jain and Miller, 1977, Petri 1977 and Maul 1985) and the properties of the receiver. For practical systems the background power on the detector is in the order of tenths of microwatts. According to the results of Austin (1981) and Spitzer and Arief (1983), the upwelling radiation from the water can be neglected in this situation. On a clear day there are two sources of background radiation viz. the sea upwelling radiation and the sun glitter. The first generates a maximum background radiance in the infrared channel of about 3.10^{-3} W/(m^2.sr.nm) and in the green channel of about 3.10^{-2} W/(m^2.sr.nm). The sun glint on the other hand depends on the direction of the sun and the viewing direction of the system. Worst case situations occur during summer under low wind speed conditions and when the system operates under off-nadir angles. Radiances of 5.10^{-2} W/(m^2.sr.nm) or higher can be expected for both channels. Under these conditions a scanning system is exposed to a change in background radiation of maximum 5 orders of magnitude which causes an enormous variation in the noise level. This problem can be taken into account by designing special detector electronics and selecting the hour of operation.

1.3 The water

Scattering and absorption of the water molecules and suspended matter play an important role in the performance of laser bathymetry systems. Values for the scattering and absorption coefficients for sea-water and the associated scattering functions are published by a.o. Jerlov and Nielson (1974, 1976), Gordon (1984), Guenther and Thomas (1981) and Jonasz (1986). Absorption only limits the penetration depth of the light in the water and thus the maximum detectable depth. Due to scattering the transmitted laser beam spreads as it propagates, thus reducing the spatial resolution. Furthermore, part of the scattered light is reflected in the direction of the receiver, thus providing information on the particle concentration as a function of depth. It must be noted that the backscatter can reach levels which are comparable with the power reflected from the bottom. As a result, the bottom reflection no longer causes a relatively strong signal at the end of the waveform. Layers and vegetation may cause false echoes and can mask the reflection from the bottom. Due to (multiple)-scattering in the water and from the wavy water surface, the signal strength from the water surface and the bottom is dependent on the field of view of the receiver. However, increasing the field of view will not only increase the signal, but will also increase the background noise and the reflected bottom pulse.

The first and higher order scattering can influence the accuracy of the depth sounding for an off-nadir pointing system, because the leading edge of the bottom reflection is determined by the shortest round trip of the photons. For a water depth of 10 m this effect can be about 50 cm as shown by Guenther and Thomas (1981).

The first order backscatter of the water can be calculated directly from the scattering properties of the suspended particles. A one dimensional approach is sufficient to model this effect. The field of view of the receiver has no influence. Higher order scattering effects - even the second order - is more complicated to calculate as shown by Dirks (1989). This must be treated spatially and is also dependent on the field of view of the receiver. Although this higher order scattering is not of direct importance on the depth accuracy, this phenomenon can be used for monitoring the water quality as proposed by Spitzer and Dirks (1988).

1.4 The bottom

Values for the diffuse reflection coefficient of the bottom sediment have been published a.o. by Clegg and Penny

(1978), Guenther and Swift (1978), Steinval (1984), Guenther (1985) and Muirhead and Cracknell (1986). Values between 5% (for mud) and 30% (for sand) are reported. The signal from the bottom can be calculated straightforward from the altitude of the sensor, the total transmission losses, the depth of the water, the diffuse reflection coefficient of the bottom, the off-nadir angle and the refractive index of water and air.

The time interval between the reflection from the water surface and the sea bottom is the key parameter for the depth of the water. The bottom reflection, however, can be masked by vegetation and contaminating layers or can totally be lost in the system noise. Furthermore no reflection at all is observed when the backscatter of the water is equal to or larger than the reflection from the bottom. It is clear that in those cases signal analysis based on pulse position identification is not adequate. Examples of original bathymetry signals have been published by Billard (1986).

1.5 Signal evaluation

A closed form analytical expression for a laser bathymetry signal cannot be given, since different media are encountered in succession. Therefore, the signal is split in an atmospheric part and a water part. For model studies, a system with a receiver area of 0.05 m^2 and a laser energy of 5 mJ in 5 ns is assumed. An example of the signal simulation is shown in Figure 3 from just above the water surface down to the bottom. Two extreme values for the atmospheric visibility and for the water attenuation coefficient are selected. In the upper curve, the atmospheric visibility is 100 km and the water attenuation coefficient is 0.1 m^{-1}. The bottom reflection is at 2.04 µs. The other curve is calculated for an atmospheric visibility of 1 km and a water attenuation coefficient of 1 m^{-1}. The simulation shows that the water attenuation coefficient can well be determined in both cases, but that in the second case the total attenuation is so strong that the reflection from the bottom is fully masked by the system noise.
The atmospheric transmission has little influence on the maximum detectable depth under operational circumstances. For a platform altitude of 300 m the maximum detectable depth decreases only 10% when the atmospheric extinction increases from 0.1 km^{-1} to 1 km^{-1}. This can be read from Figure 4.

The water attenuation coefficient, however, has a strong influence on the maximum detectable depth. This effect is show in Figure 4 for three different values of the noise equivalent power. For a practical system (NEP=10^{-8} W) at

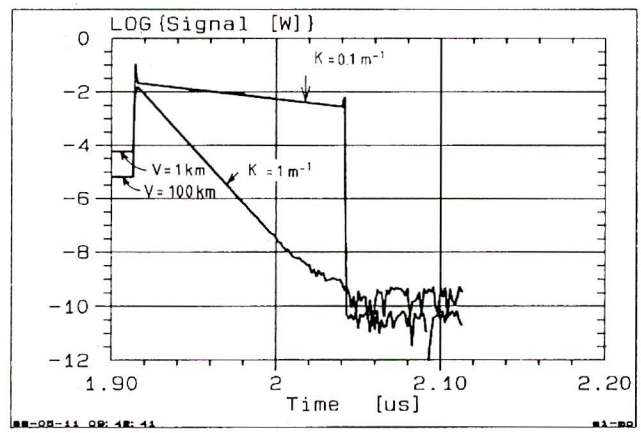

Fig. 3 - Calculated bathymetry signals for two different atmospheric visibilities and two different values of the water attenuation coefficient.

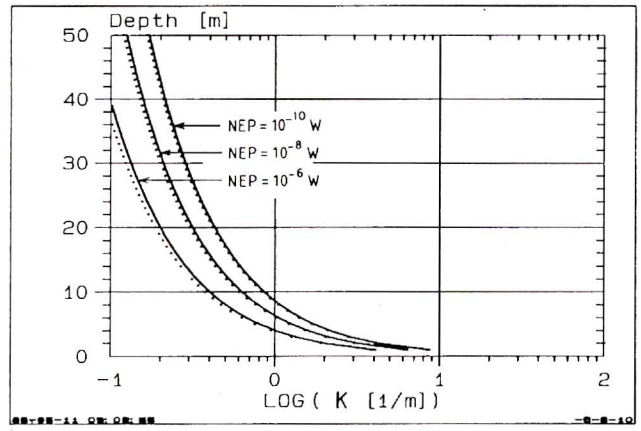

Fig. 4 - Maximum detectable depth as a function of the water attenuation coefficient C_w for a platform altitude of 300 m, an atmospheric extinction coefficient of 0.1 km^{-1} and three values of the background noise. The dotted curves are for an atmospheric extinction coefficient of 1 km^{-1}.

an altitude of 300 m the maximum detectable depth decreases from about 60 m to about 6 m when the water attenuation coefficient increases from 0.1 m^{-1} to 1 m^{-1}.

For large water attenuation coefficients an increase of the system sensitivity (combination of laser energy, sensitivity of the receiver and noise of the receiver) will increase the maximum measurable water depth only slightly. For example when the water attenuation coefficient is 2 m^{-1}, the maximum detectable depth increases only from 2 m to 5 m when the system sensitivity increases over 5 orders of magnitude! The increase in system sensitivity is more efficient in situations of low water attenuation coefficients. This effect is shown in Figure 5 were the maximum detectable depth has been plotted as a function of the system sensitivity for different values of the water attenuation coefficient.

The altitude of the platform has only effect on the maximum detectable depth in situations of low (0.1 m^{-1}) water attenuation coefficients. When the platform rises from 100 m to 1000 m, the maximum detectable depth reduces about 20%. For large values of the water attenuation, the altitude of the platform has almost no influence on the maximum detectable depth. The results of the model simulations are shown in Figure 6 were the maximum detectable depth has been plotted as a function of the platform altitude.

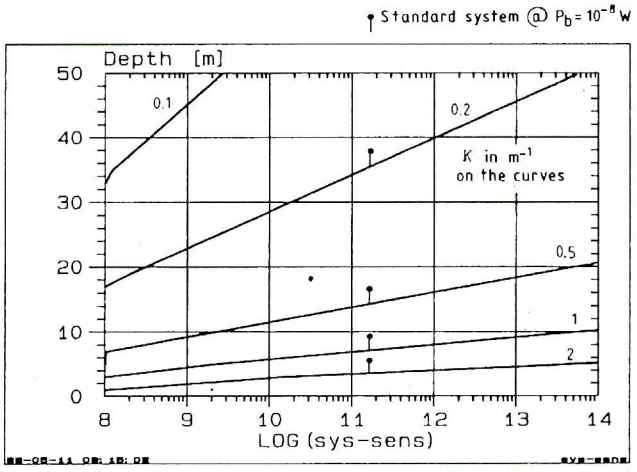

Fig. 5 - Maximum detectable depth as a function of the system sensitivity (see text). The water attenuation coefficient has been parameterized.

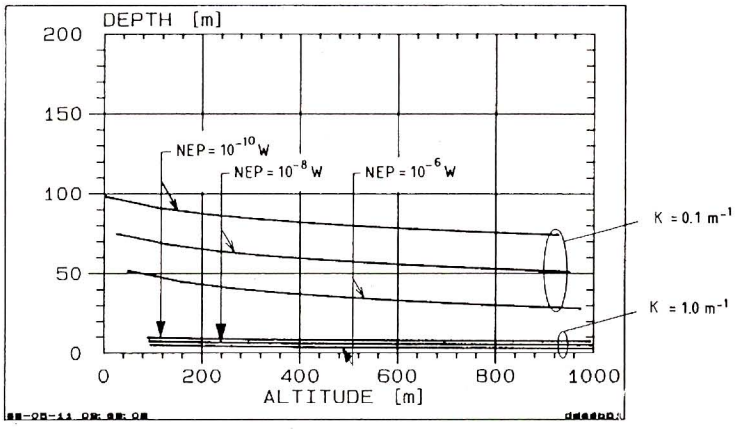

Fig. 6 - Maximum detectable depth as a function of the altitude of the platform for two different values of the water attenuation coefficient and three value of the system noise equivalent power.

2. HARD AND SOFTWARE

An opto-mechanical system has been proposed which consists of a laser, a main scanning lidar unit and a small fixed lidar unit. The fixed unit measures the average sea level altitude. The main unit, with two rotating wedges, has been proposed by Visser and Smorenburg (in Dirks, 1989). The rotating direction and phase shift between the two wedges determine the scan pattern. The whole system must be mounted on a roll-stabilized platform. Other hardware includes detectors with different field of views, beam splitters, lenses and optical filters for the appropriate wavelength selection.

Digital and analog data processing are necessary, both in flight and after flight, to control the system and to store the measured data (Van Mierlo and De Vries in Dirks, 1989). Additional information, like position, time and speed of the platform, must be stored simultaneously with each sounding. Although much of this process can be performed with standard instrumentation, the user requirements need special processing of the data. The amount of software development should not be underestimated (Childs and Enabnit 1982) and may be comparable to the manpower needed for the construction of the opto-mechanical part.

CONCLUSIONS

The feasibility study shows that laser bathymetry is a complex optical remote sensing technique with many aspects, each requiring detailed consideration. Crucial are the water surface, the properties of the water itself and to a lesser extent the background radiation on clear days. The atmospheric properties and the reflection properties of the bottom are less difficult to treat. It was recommended to realize such a system in small steps and in modules. In such a way separate aspects of the whole system can be studied separately. Apart from depth soundings, laser bathymetry systems can also be applied for the investigation of the scattering properties of the water and the properties of the water surface.

Simple water surface simulations and ray tracing techniques show the large influence of the water surface on beam spread and shape of reflected laser pulses. The performance of the system has been simulated as a function of the system sensitivity, the altitude of the platform and the water attenuation coefficient.

APPENDIX

Atmospheric background in a nadir looking receiver.

Assume an optical receiver with an area of A_r (m^2) and field of view of θ_r (rad). The irradiance by the sun is E_o ($Wm^2 \cdot nm$). The aerosols are represented by the backscatter coefficient β_a (km^{-1}) and extinction coefficient σ_a (km^{-1}).

Consider and elementary volume dV at a range R from the receiver. The backscatter from this volume is detected by the receiver under nadir angle ϕ at an altitude h. The volume has a thickness of dh and is limited by the angle between ϕ and $\phi + d\phi$.

The volume dV can be written as:

$$dV = 2\pi \cdot h^2 \cdot dh \cdot \sin(\phi) \cdot d\phi / \cos^3(\phi)$$

Considering that R=h/cos(ϕ) gives:

$$dP_{sc} = 2\pi \cdot E_{su} \cdot \beta_a \cdot A_{rec} \cdot dh \cdot \tan(\phi) \cdot d\phi \cdot$$

$$\cdot \exp(-2 \cdot \sigma_a \cdot h / \cos(\phi)) .$$

Integrating both over h and ϕ (assuming that θ_r is small) results in:

$$P_{sc} = \pi \cdot E_{su} \cdot A_{rec} \cdot \beta_a / \sigma_a \cdot ln \{ sec(\theta_\tau / 2) \} \cdot$$

$$\cdot \{ 1 - \exp(-2 \cdot \sigma_a H) \} .$$

REFERENCES

Austin, R.W., 1981, Remote sensing of the diffuse attenuation coefficient of ocean water. AGARD Electromagnetic Wave Propagation Panel, Monterey, USA, 6-10 April.

Bobb, L.C. et al., 1979, Capillary wave measurements. Appl. Opt. Vol. 18, No. 8, 1167.

Bucher, E.A., 1973, Experiments on light pulse communication and propagation through atmospheric clouds. Appl. Opt., Vol. 12, No. 10, 2401.

Chang, J.H. et al, 1978, Measurement of height frequency capillary waves on steep gravity waves. J. of Fluids Mech. Vol. 86, part 3, 401.

Childs, J.D. and D.B. Enabnit, 1982, User requirements and a high level design of the hydrographic software/data processing subsystem of an airborne laser hydrography system. NOAA Technical Report OTES 11, Rockville, Md, USA.

Clegg, J.E. and Penny, 1978, Depth sounding from the air by laser beam. J. Navig. Vol. 31, 52.

Cox. C and W. Munk, 1954, Slopes of the sea surface deduced from photographs of sun glitter. Bull. Scripps Inst. Un. Cal. Vol. 6, No. 9.

Dirks, R.W.J. et al, 1989, Pre-study laser bathymetry. BCRS, Netherlands remote sensing board, P.O. Box 5023, 2600 GA Delft, Report BCRS-89-26.

Gordon, R. et al, 1984, Introduction to ocean optics. SPIE Vol. 489, Ocean Optics.

Guenther, G.C. and R.N. Swift 1978, Laser bathymetry for near shore chartering applications. Oceans, 78, New York, IEEE, 390.

Guenther, G.C. and R.W.L. Thomas, 1981, Monte Carlo simulations of the effects of underwater propagation on the penetration and depth measurements bias of an airborne laser bathymeter. NOAA Technical Memorandum OTES 01, Rockville Md. USA.

Guenther, G.C., 1985, Airborne laser hydrography. NOAA Professional Paper Series, National Ocean Series 1, Rockville, Md. USA.

Haimbach, S.P. and J. Wu, 1986, Directional slope distributions of wind-disturbed water surface. Radio Science, Vol. 21, No. 1, 73.

Hughes, H.G., 1984, Estimates of optical pulse broadening in maritime stratus clouds. Opt. Eng., Jan/Febr., Vol. 23, No.1 ,38.

Jain, S.C. and J.R. Miller, 1977, Algebraic expression for the diffuse irradiance reflectivity of water from the two flow model. Appl. Opt., Vol 16, No. 1, 202.

Jerlov, N.G. and E.G. Nielson. 1974, Optical aspects of oceanography. (New York, Academic Press).

Jerlov, N.G., 1976, Marine Optics. (Amsterdam, Elsevier Oceanography Series 14).

Jonasz, M., 1986, Comparison of measured and computed light scattering in the Baltic. Tellus, 38B, 144.

Matter, J.C., 1981, Optical pulse propagation through clouds. Appl. Opt., Vol. 20, No. 4, 544.

Maul, G.A., 1985, Introduction to satellite oceanography. (Dordrecht, Martinus Nijhoff).

Mc.Clain C.R., et al, 1982, Measurements of sea state variations across oceanic fronts using laser profilometry. J. of Phys. Ocean. Vol. 12, 1228.

Muirhead, K and A.P. Cracknell, 1986, Airborne lidar bathymetry. Int. J. Remote Sensing, Vol. 7, No. 5, 597.

Petri, K., 1977, Laser radar reflectance of Chesapeake Bay waters as a function of wind speed. IEEE Trans. Geoscience Electronics, GE-15, No. 2, 87.

Schau, H.C., 1978, Measurement of capillary wave slopes on the ocean. Appl. Opt. Vol. 17, No. 1, 15.

Spitzer, D and R.W.J. Dirks, 1988, Laser remote sensing of particle concentration in sea-water. Private communication.

Spitzer, D. and D. Arief, 1983, Relationship between the sky radiance at the sea surface and the downwelling irradiance. Appl. Opt. Vol. 22, No. 3, 378.

Steinval, O. a.o., 1984, Advanced technology for hydrography mapping. FOA Report C 30371-EL September, Linkoping, ISSN 0347-3708.

Stotts, L.B., 1978, Closed form expression for optical pulse broadening in multiple-scattering media. Appl. Opt., Vol. 17, No. 4, 504.

Wu, J., 1971, Slope and curvature distributions of wind disturbed water surface. J.O.S.A. Vol. 61, No. 7.

Zaha, M.A., 1972, Shedding some needed light on optical measurements. Electronics, 6, 91.